Mixed-Matrix Membranes for CO_2 and H_2 Separations Using Metal-Organic Frameworks and Mesoporous Hybrid Silicas

Edson V. Perez, Yanfeng Zhang, Ma. Josephine Ordoñez, Kenneth J. Balkus Jr., John P. Ferraris, and Inga H. Musselman

Department of Chemistry and The UTD NanoTech Institute, The University of Texas at Dallas, Richardson, TX 75083-0688, USA

Introduction

Industrial applications of membranes in many gas separations continue to grow. Current polymeric membrane materials have seemingly reached a limit in the tradeoff between permeability and selectivity [1]. Therefore, recent research efforts have focused on synthesis and evaluation of novel materials that could enhance the separation and gas transport properties of membranes. Mixed-matrix membranes (MMM) that incorporate new microporous materials such as metal-organic frameworks (MOF) have the potential to achieve DOE goals for targeted separations (Figure 1). Metal-organic frameworks are microporous materials that have high gas storage capacities due to their high surface area. For example, MOF-177 has a high CO_2 storage capacity [2]; Cu-MOF, Cu-BPY-HFS have high CH_4 uptake [3,4]; MOF-5 has high H_2 sorption; IRMOF-6 and IRMOF-8 have 2 and 4 more times the H_2 storage capacities of MOF-5 under the same conditions [5]. Cu-DHBC-BPY exhibits selective adsorption of gases depending upon the pressure [6]. The organic character of the MOFs make them more compatible with the polymer matrix thereby reducing defects caused by poor wetting/phase separation. For MOP-18 (Figure 1c) [7], the organic component of the MOF makes it soluble in organic solvents resulting in better membrane fabrication. Other novel materials, such as carbon aerogel-zeolite composites, with both micro and mesopores, which can provide better interfacial contact [8] and SWNTs that allow ultrafast diffusion [9] were also investigated in this project.

Experimental

MOF synthesis: Cu-MOF, MOF-5, and MOP-18 nanocrystals were synthesized by modifying literature procedures [3, 11, 7]. Crystal activation by solvent exchange (chloroform and acetone), followed by high temperature drying, was performed in order to empty the pores of the crystals. ZIF-8 nanocrystals were synthesized by modifying Yaghi's procedure [10] by adding an amine and activation with methanol.

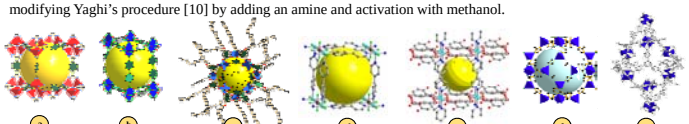

Figure 1. Crystal structures from single crystal and theoretical (*th*) diffraction patterns of a) MOF-5 [5], b) Cu-MOF (*th*) [3], c) MOP-18 [7], d) HFS-BiPy [4], e) BiPy [6], f) ZIF-8 [10], and g) MOF-177 [2]

MOF/Matrimid® membrane fabrication: MOF nanocrystals were dispersed in chloroform by sonicating for 6 hours and stirring for one day; MOP-18 nanocrystals immediately dissolved in chloroform without sonication. Matrimid® was dissolved in chloroform and stirred for one day before the MOF solution was added. 0%, 10%, 20%, and 30% (w/w) MOF/Matrimid® membranes were cast on Mylar® A92 films. The MOF-5/Matrimid® membranes were annealed at 240 °C in a vacuum oven for 1 d. The Cu-MOF/Matrimid® and the MOP-18/Matrimid® membranes were annealed at 150 °C for 10 h. Permeation, XRD, TGA, and SEM analysis/imaging were performed on the membranes.

Permeability studies: Single gas permeabilities were evaluated for H_2, O_2, N_2, CO_2, and CH_4 using a custom-built gas permeameter equipped with a 1-200 amu RGA [12].

Results and Discussion

Mesoporous Hybrid Silicas

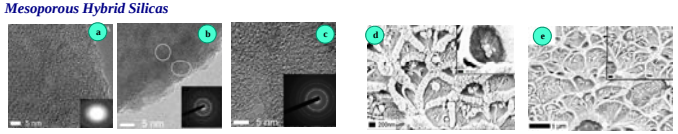

TEM images of (a) carbon aerogel and (b) carbon aerogel-zeolite A and (c) carbon aerogel-zeolite Y composite

Cross-section of 10 wt % carbon aerogel and 10 wt % carbon aerogel-zeolite A-Matrimid membranes

Figure 2. TEM and SEM images of carbon aerogel and carbon aerogel–zeolite composite

TEM shows zeolite lattice fringes in the amorphous carbon aerogel. SAED also shows the presence of crystalline materials (Figure 2). XRD patterns show characteristic zeolite A and zeolite Y peaks (Figure 3). The BET surface area and pore size distribution of carbon aerogel-zeolite composites are similar to carbon aerogel (Figure 4).

Compared to the pure polymer, pure gas permeation tests of 10% (w/w) carbon aerogel-zeolite A/Matrimid® membranes show higher selectivity toward O_2/N_2 (9.3), H_2/N_2 (120.6), CO_2/CH_4 (71.5) and H_2/CH_4 (172) compare to Matrimid® [O_2/N_2 (6.6), H_2/N_2 (79.6), CO_2/CH_4 (34.7) and H_2/CH_4 (83.3)]. The carbon aerogel-zeolite Y/Matrimid® membranes provided similar results (Fig 5). The presence of micropores (from both carbon aerogel and zeolites) can provide size and shape selectivity for gas separation. The low cost of carbon aerogels is especially promising for industrial applications.

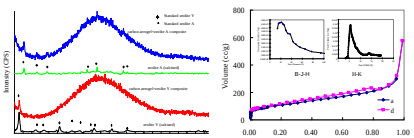

Fig 3. XRD patterns of carbon aerogel-zeolite composites

Fig 4. N_2 adsorption- isotherm of carbon aerogel
BET area= 344 m^2/g, pore size: 0.53 nm and 2.14 nm

Single Wall Carbon Nanotubes

SWNT functionalized with carboxylic groups and short SWNT were incorporated into Matrimid to form mixed matrix membranes. Pore diameter of the SWNTs is around 1.0 nm. Pure gas and gas mixture separation shows that there is no change in selectivity, while the permeability increases by at least 30% (Fig 6). The increase in permeability can be attributed to the fast diffusion inside the SWNTs.

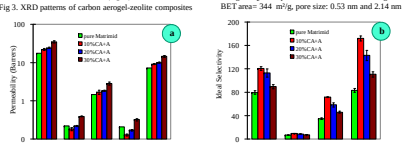

Fig 5. Gas permeabilities and ideal selectivities of carbon aerogel-zeolite A-Matrimid® membranes.

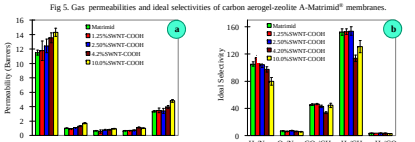

Fig 6. Gas permeabilities and ideal selectivities of SWNT-COOH-Matrimid® membranes.

Metal-Organic Frameworks

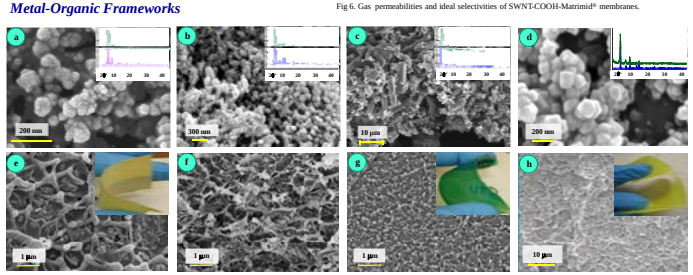

Figure 7. Crystal SEM images and XRD [insets: experimental (green) and theoretical (blue)] of activated a) MOF-5, b) Cu-MOF, c) MOP-18, and d) ZIF-8 crystals. Membrane cross-section SEM images of 20% (w/w) MOF/Matrimid® of: e) MOF-5, f) Cu-MOF, g) MOP-18, and h) ZIF-8 mixed-matrix membranes.

XRD patterns of the activated MOF-5, Cu-MOF, MOP-18, and ZIF-8 nanocrystals (insets of Figure 7 a,b,c,d respectively) show good agreement with the published theoretical diffraction patterns showing the integrity of the crystals after pore evacuation. SEM images show aggregates smaller than 100 nm for MOF-5, Cu-MOF, and ZIF-8 (Figure 7 a,b,d). The SEM image of MOP-18 (Figure 7c), however, shows large aggregates in a rectangular shape morphology, despite the fact that these aggregates dissolve readily in chloroform. From N_2 sorption isotherms at 77 K, HK pore sizes of MOF-5 and Cu-MOF were calculated (0.8 nm and 1.0 nm respectively) which were similar to the ones reported by Yaghi and Seki [3,13]. Obtained BET surface areas follow a similar trend (MOF-5 = 2400 m^2/g, Cu-MOF = 3300 m^2/g). Permeability experiments with MOF-5/Matrimid® MMMs show that the MOF-5 exerts a positive effect on H_2 permeability (Figure 8a); a 120% increase in permeability at 30% (w/w) MOF-5 and no significant variation in selectivity. Cu-MOF/Matrimid® MMMs shows similar effect but with a large increase in permeability for H_2 (900% increase) and improved selectivity for methane. A 3100 % increase in permeability for methane was achieved when compared to Matrimid® (Figure 8b). MOP-18/Matrimid® MMM also shows impressive permeability and selectivity values (Figure 8c), and this membrane was shown to be selective for methane with a 200% increase in permeability (0.50 Barrers for MOP-18/Matrimid® and 0.24 Barrers for Matrimid®). For mixed gas separation, CH_4/N_2 selectivity improved by 300% when using the 20 wt% Cu-BPY-HFS and Cu-DHBC-BPY/Matrimid MMMs (Table 1 and Table 2).

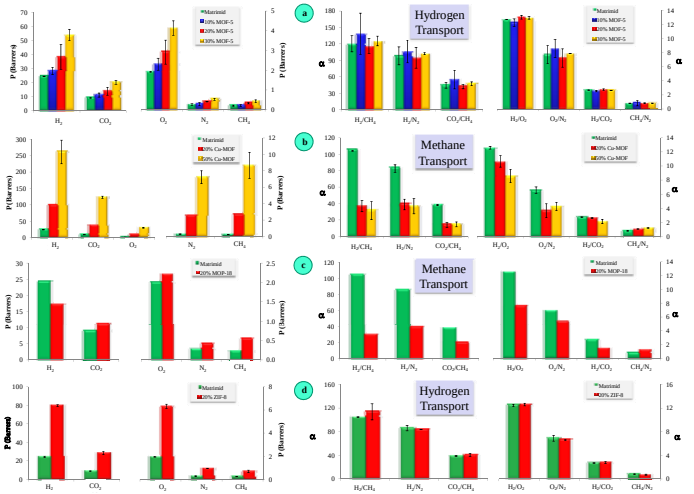

Figure 8. Permeabilities and selectivities of different gases of a) MOF-5/Matrimid® membranes at different MOF-5 loadings, b) Cu-MOF/Matrimid® at 20% and 50% (w/w) loadings, and c) MOP-18/Matrimid® at 20% (w/w) loading, and d) ZIF-8/Matrimid® at 20% (w/w) loading.

Table 1. Gas mixture separation using Cu-BPY-HFS-Matrimid membranes (at 35 ° C)

Selectivity	Mixture (mol%)	Matrimid	20% Cu-BPY-HFS-Matrimid	
CH_4/N_2	94% CH_4/ 6% N_2	0.95	3.21	Ideal selectivity 1.16
	50% CH_4/ 50% N_2	0.90	3.52	
	25% CH_4/ 75% N_2	0.91	3.76	
CO_2/CH_4	75% CO_2/ 25% CH_4	34.3	10.32	Ideal selectivity 27.62
	50% CO_2/ 50% CH_4	32.3	11.23	
	10% CO_2/ 90% CH_4	36.5	10.54	

Table 2. Gas mixture separation using Cu-DHBC-BPY-Matrimid membranes (at 35 ° C)

Selectivity	Mixture (mol%)	Matrimid	20% Cu-DHBC-BPY-Matrimid	
CH_4/N_2	94% CH_4/ 6% N_2	0.95	3.47	Ideal selectivity 1.11
	50% CH_4/ 50% N_2	0.90	3.33	
	25% CH_4/ 75% N_2	0.91	4.35	
CO_2/CH_4	75% CO_2/ 25% CH_4	34.3	16.53	Ideal selectivity 23.45
	50% CO_2/ 50% CH_4	32.3	13.56	
	10% CO_2/ 90% CH_4	36.5	14.24	

Conclusions

The successful incorporation and performance of MOF nanocrystals in mixed-matrix membranes show that these materials have great potential in gas separations. Increased permeabilities and selectivities for target gases like hydrogen and methane have been achieved with zinc and copper based MOFs, respectively. Hydrogen and methane permeabilities increased due to greater solubility of these target gases in the mixed-matrix membrane. Higher selectivity for carbon aerogel-zeolite composite membranes can be attributed to better interfacial contact and selective adsorption.

References

1. Robeson, L. M.; *J. Membr. Sci.*, **1991**, 62, 165.
2. Millward, A.; Yaghi, O. M.; *J. Am. Chem. Soc.*, **2005**, 127 *(51)*, 17998.
3. Seki, K., *Chem. Commun.*, **2001**, 1496.
4. Norn, S. I.; Kitagawa, S.; Kondo, M.; Seki, K. *Angew. Chem. Int. Ed.* **2000**, 39, 2081-2084.
5. Yaghi, O. M.; Rosi, N. L.; Eckert, J.; Eddaoudi, M.; Vodak, D. T.; Kim, J.; O'Keefe, M., *Science*, **2003**, 300, 1127.
6. Kitaura, R.; Seki, K.; Akiyama, G.; Kitagawa, S. *Angew. Chem. Int. Ed.* **2003**, *42*, 428-431.
7. Yaghi, O. M., *J. Am. Chem. Soc.* **2006**, 128, (26), 8398.
8. Schuth, F.; *Chem. Mater.*, **2004**, 16(26), 5676 -5681.
9. Chen, H.; Sholl, D. S.; *J. Am. Chem. Soc.* **2004**, *126*, 7778-7779.
10. Park, K. Y.; Ni, Zheng; Cote, A. P.; Choi, J. Y.; Huang, R.; Uribe-Romo, F. J.; Chae, H. K.; O'Keeffe, M.; Yaghi, O. M., *PNAS* **2006**, *103*, 10186.
11. Huang, L.; Wang, H.; Chen, J.; Wang, Z.; Sun, J.; Zhao, D.; Yan, Y., *Micropor. Mesopor. Mat.*, **2003**, 58, 105.
12. Reid, B.; Ruiz-Trevino, F. A.; Musselman, I. H.; Balkus Jr., K. J.; Ferraris, J. P., *Chem. Mater.*, **2001**, 13 *(7)*, 2366.
13. Eddaoudi, M.; Kim, J.; Rosi, N.; Vodak, D.; Wachter, J.; O'Keefe, M.; Yaghi, O. M., *Science*, **2002**, 295, 469.

Acknowledgments

U.S. Department of Energy, Grant # DE-FG26-04NT42173